

Effect of Point Defects on the Structural and Optical Properties of CdS Nanoparticles Synthesized by Chemical Method

Rand Rasim Alani^{1, a*} and Omar Adnan Ibrahim^{1, b}

¹University of Baghdad, Collage of Science, Physics Department, Baghdad, Iraq

Keywords: Nanoparticles, CdS, UV–Vis absorption, Photoluminescence, Defects, surface states, defects scheme.

Abstract

In this study, cadmium sulfide (CdS) Nanoparticles (NPs) are synthesized by a chemical method. Also, by subjecting the CdS nanoparticles to a rapid cooling, the point defects have been synthesized. Our objective is to synthesize point defects in CdS nanoparticles in order to study their effect on the Structural, Morphological, and Optical Properties. To determine the crystallographic structure in CdS thin films, XRD measurements have been carried out. The Transmission Electron Microscopy (TEM) was used to observe CdS NPs size. The outcome images reveal that the CdS NPs are approximately (5 nm) in size. Also, Ultraviolet-visible (UV–Vis) absorption spectroscopy was used to calculate the material's band gap and showed an absorption peak at 419 nm ~ (3 eV), indicating a blue shift of 0.6 eV compared to bulk CdS. By utilizing the X-ray diffraction patterns (XRD), the particles size was found to be at 4.8 nm. Multiple cadmium and Sulfur defects were observed by employing the photoluminescence (PL) method. A decrease of PL intensity in CdS film was detected due to defects recombination. The results indicate that Cd interstitials (I_{Cd}) and Cd vacancies (V_{Cd}) are active defects, which act as double donors and double acceptors, respectively. The FTIR spectroscopy studies effectively identified the synthesized compound's functional groups and determined the molecular structure. At the end, an easy to read scheme for most of the defects transitions that may happen was plotted.

Introduction

In the last two decades, the interest in the physical, optical, and transport properties of nanometer-sized semiconductor particles or quantum dots has increased. There are unique optical and electrical properties for semiconductor nanoparticles that are significantly different from the corresponding bulk depending on the quantum confinement effect. When the dimension of the semiconductor quantum dots approaches the Bohr exciton radius, considerable changes in their properties occur. Accordingly, the surface-to-volume ratio changes and the electronic energy levels shift towards higher energy, increasing the band gap [1, 2].

This increase allows researchers to use it in optoelectronic and piezoelectric devices [3, 4, 5], photodegradation [6], and light-emitting diodes [7]. Cadmium sulfide (CdS) is a widely studied semiconductor, that has been used in photodetectors, optoelectronics, and for solar cell applications as a window layer of type-n because of its wide direct band gap (2.42 eV) [8]. Cadmium sulfide can exist mainly in two crystalline phases, hexagonal wurtzite, and cubic zinc-blende, depending on the preparation conditions [9].

The optical properties of semiconductor nanocrystallite are highly dependent on its crystalline structure. In other words, the effective masses of electrons and holes in their electronic bands can be noticeably changed due to crystalline phase differences. The cubic phase of CdS is kinetically controlled. In comparison, the hexagonal phase of CdS is thermodynamically controlled [10]. Consequently, researchers prefer a reaction that forms thermodynamically stable nanoscale CdS materials.

The evolution of defects such as S-vacancies, Cd-vacancies, and Cd-interstitials complexes, is addressed when discussing the electrical and optical properties of CdS. Where the V_{Cd} can be defined as the process of missing the Cd atoms in its position, leaving behind a void, and I_{Cd} are the Cd atoms that replace some of the S atoms. This article characterizes some trap and deep levels of CdS, including different convenient characterization techniques. Moreover, studying the evolution of such defects in the b-CdS to a-CdS transformation.

In order to understand the phenomena occurs in semiconductor nanoparticles, it is important to use a suitable method for their preparation. Among the various synthesis techniques, chemical synthesis methods are promising in terms of cost reduction and the ability to produce large amounts of particles. In general, the chemical method consists of the reaction of Cd and S compounds. Moreover, since it is an easy way to stabilize the nanoparticles and avoid the agglomeration, different organic molecules are used.

Experimental Work

In this work, we studied the optical, electrical, and structural properties of the CdS by preparing its nanoparticles utilizing a chemical method.

A. Synthesization of Cd

Copyrights @Kalahari Journals

Vol. 7 No. 1 (January, 2022)

International Journal of Mechanical Engineering

In order to prepare the Cd solution, we dissolved cadmium chloride ($CdCl_2 \cdot 5/2 H_2O$) as cadmium ions source into Oleylamine using a flask subjected to a magnetic stirring at 90 °C for 30 min while the flask neck is closed.

B. Synthesize of Sulphide S

For preparing Sulphide S, 0.048 g of Sulfur S was dissolved as a source of Sulphide ions into 10 ml of Oleylamine at 40 °C until its color changed from yellow to red. Then after the temperature of cadmium chloride solution was raised to 175 °C, the sulfide solution was gradually added to the cadmium chloride solution and stirred for 6 hr before cooling the mixture. The high purity nanoparticles of CdS were obtained by adding the mixture to ethanol and separated the yellow precipitate away from the solution through the centrifugation process and drying. By doing this separation process, the yellow precipitate is ready for use in measurements.

To obtain structural properties, the X-ray diffraction (Cu radiation, 1.5406 °Å) was used. Then, the crystallite size was calculated by Williamson-Scherrer's formula. Moreover, the surface images of CdS nanoparticles were obtained through a Scanning Electron Microscopy SEM and the morphological properties were measured by transmission electron microscope. Also, utilizing UV–Vis absorption spectroscopy, the optical properties were identified. Finally, for the photoluminescence (PL) experiment, the excitation was obtained by the UV lines from a 200W mercury arc lamp source.

Results and discussion:

X-ray diffraction pattern

In order to identify the structural and crystalline phases, XRD was performed for the prepared samples using $CuK\alpha$ ($\lambda= 1.5406 \text{ \AA}$) radiation source.

Fig. 1 shows the formation of XRD pattern for the obtained CdS nanoparticles. The crystal phase of the product was determined to be wurtzited structure that having hexagonal phase. It shows that CdS nanoparticles has six peaks at the angles of 25°, 26.5°, 28.3°, 44°, 48°, and 52°. These results correspond to the Miller indices for the crystalline plane of [100], [002], [101], [110], [103], and [112], respectively. The diffractogram illustrates that hexagonal crystalline phase occurs according to the standard reference (JCPDS 01-080-0006).

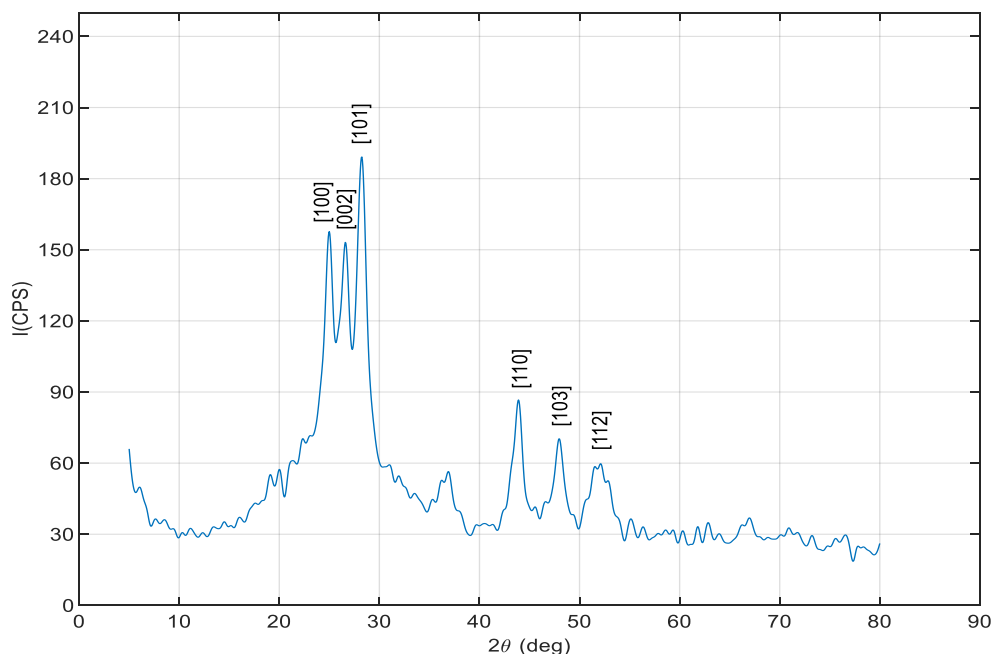


Fig. 1: XRD pattern of Cadmium sulphide nanoparticles

As it is shown in Fig. 1, the X-ray peak intensities are sharp and narrow at angles ($2\theta = 25^\circ, 26.5^\circ$ and 28.3°) which suggest that the crystal is polycrystalline.

By utilizing the peak width, the average sizes of the nanocrystals can be estimated using Debye-Scherrer equation [11, 12].

$$D = K\lambda / \beta \cos \theta \quad (1)$$

Where K is a geometrical factor, D is the average particle size, λ is the wavelength of X-ray radiation, β is the full width at half maximum (FMWH) of the peak, and θ is the diffraction angle (Bragg diffraction angle). The resulted average crystal size of the CdS nanoparticles is $D = 4.8$ nm. This is close to that obtained by TEM. The broadening of the diffraction peak of XRD spectra in CdS nanoparticles occurred due to the defects as well as the crystallite size, and lattice strain which happens as result of quantum confinement effect [13]. In order to obtain these parameters, the Williamson-Hall and Scherrer methods were applied, by using the formula:

$$\beta_m \cos \theta = \frac{0.9\lambda}{d} + 4\eta \sin \theta \quad (2)$$

Where $\beta_m \cos \theta$ represent the total broadening, η is the lattice strain. So, by plotting $\beta_m \cos \theta$ against $4\sin\theta$, a straight line and intercept $0.9\lambda/d$ were gotten. Thus, the strain and particle size are calculated from the slope and y-intercept of the fitted line respectively, as shown in Fig. 2

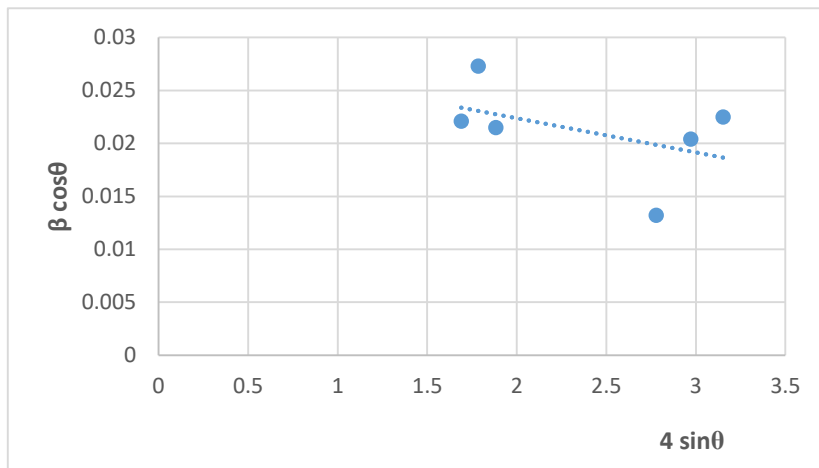


Fig. 2: Size and Strain analysis plot of CdS nanoparticles

Table 1, shows the data obtained from the Scherrer's formula and the Williamson-Hall plot W-H.

Table 1: The data of broadening the peak that due to the particle size and lattice strain

2θ	hkl	$4 \sin\theta$	$\beta \cos\theta$	d (nm)	W-H
25	100	1.6904	0.0221	6.244343891	6.249753171
26.5	002	1.7848	0.0273	5.054945055	5.060656415
28.3	101	1.884	0.0215	6.418604651	6.424633451
44	110	2.7784	0.0132	10.45454545	10.46343633
48	103	2.9724	0.0204	6.764705882	6.774217562
52	112	3.152	0.0225	6.133333333	6.143419733

Scanning Electron Microscopy (SEM)

Using Scanning Electron Microscope (SEM) along with Transmission Electron Microscopy (TEM), the surface morphology of the synthesized CdS nanoparticles was investigated. The SEM images of CdS nanoparticles of (100) kx enlargement, as demonstrated in Fig. 3, show that there are particles forming massive, approximately spherical, agglomerations. This result is in close agreement with Devi [14]. At the same time, the enlarged image shows a collection of non-uniform particles that known as a crystal size, agglomerated randomly in the range of 200 nm.

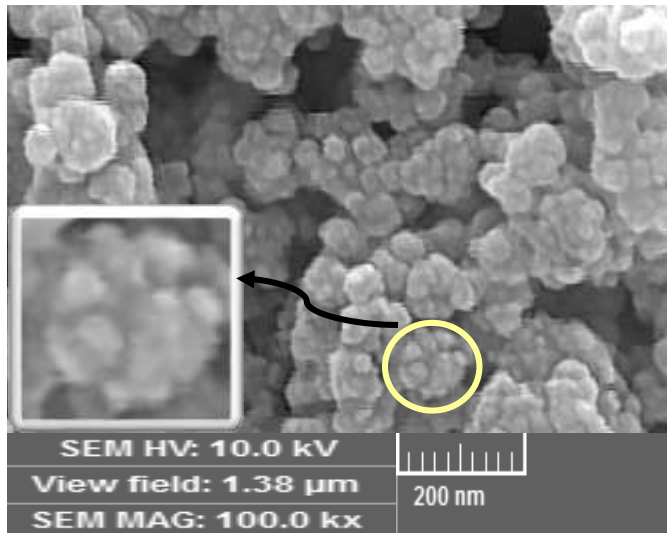


Fig. 3: SEM images of synthesized CdS nanoparticles.

Transmission Electron Microscopy (TEM)

To obtain more accurate structural for CdS nanoparticles, the Transmission Electron Microscopy was utilized. The exact particle size of CdS was determined by utilized TEM images as shown in Fig.4.

By using a high-resolution TEM image with scale factor of 50 and 100 nm, the particles size of the synthesized nano-CdS was approximately 5 nm. This result coincides with the results of grain size of CdS estimated from XRD. Fig. 4 shows the two images of TEM.

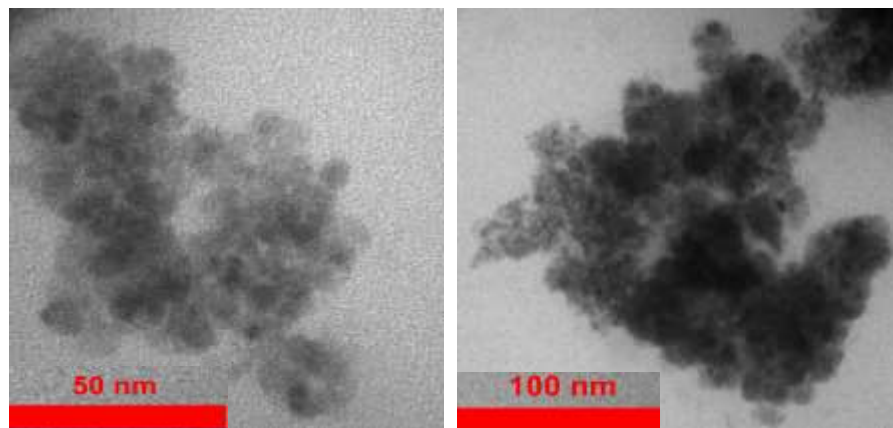


Fig. 4: TEM images of CdS nanoparticles with two different magnification powers.

UV-Visible analysis:

The UV-Visible absorption spectra and the transmittance spectra of the synthesized CdS nanoparticles have been studied by the absorption of electromagnetic radiations process as shown in Fig 5. The range of wavelength absorption spectra and the transmittance spectra of the synthesized CdS nanoparticles were allocated to be between 290-800 nm. From the absorption spectrum of CdS nanoparticles, the uttermost absorption was observed at 290 nm which correspond to the transitions from lowest level of valance band to the highest level in conduction band as a result of rotational and vibrational levels which participate in the absorption process. Moreover, we observed that when the transitions approached the two edges of energy band gap, the probability of absorption decreases, see Fig. 5.

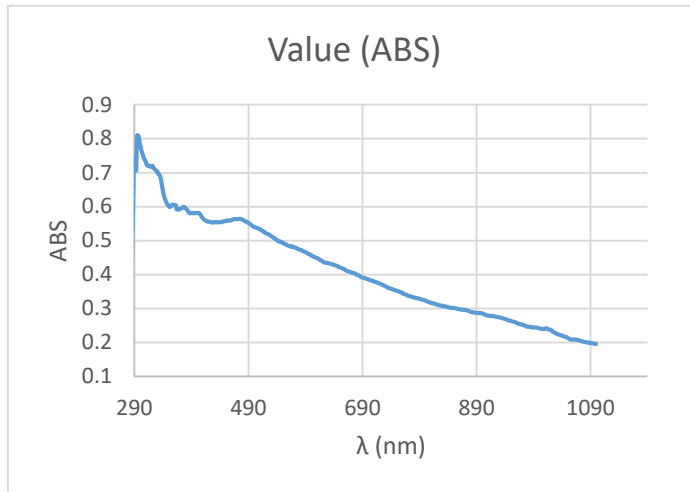


Fig. 5: UV-vis absorption spectrum of CdS nanoparticles.

Also, two peaks absorption regions were appeared at 364 and 385 nm wavelengths. This is due to the transitions that occurs between the two bands as a result of the defects ($V.B-I_{cd}$) [15]. There was a wide absorption peak appears at 490 nm, which is assigned to the transitions that occurs between cadmium interstitial and cadmium vacancy ($I_{cd}-V_{cd}$) complexes and they are majority. The I_{cd} defect formed band, that is closed to conduction band, thus, the absorption peak pop up. This result corresponding with the results reported by Elilarassi et al. [16], and Waly et al. [17]. The estimated optical band gap value of the as-prepared nanoparticles is 412 nm~(3 eV). This is higher than the band gap value (2.4 eV) of bulk CdS [18, 19, 20]. The blue shift in band gap due to the quantum confinement is approximately 0.6 eV. This increasing in the band gap happened due to reduce the particle size (nanocrystal size) of the synthesized CdS nanoparticles resulted from the quantum confinement effect, since the emission wavelength shifts towards higher energies (lower wavelengths) [17].

PL measurement

In the luminescence process, emission of semiconducting materials originates from electrons in the conduction band, trap states, crystal defect states and excitonic states [21, 9]. The Photoluminescence spectra of prepared CdS is presented in Fig (6).

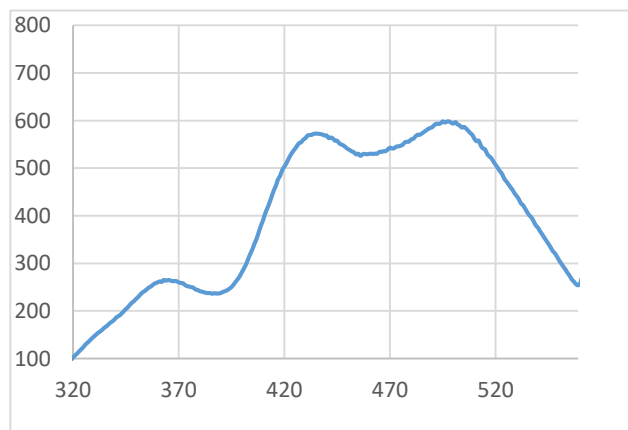


Fig 6: Photoluminescence spectra of CdS NPs

The highest wavelength of absorbance (290 nm) is used to excite the sample in which the emission spectrum shows a peak at (430 nm). According to studies on photoluminescence of CdS nanoparticles, the emission happens due to band edge and imperfections [22, 23, 24]. Therefore, the emission peak observed at 430 nm (2.8 eV) in the PL spectra of CdS nanoparticles can be attributed to the surface state (S.S) emission, which is defined as the radiative recombination of exciton on the surface of NPs. where the PL peak energy of such surface state emission, in general, is lower than the band gap energy of nanoparticles.

To find this blue shift in the band gap energy of the nanoparticle relative to the bulk material, the following equation was used [25]:

$$\Delta E = E_{np} - E_{bulk} = \frac{hc}{\lambda} - E_{bulk} \dots\dots\dots (2)$$

Where E_{np} , E_{bulk} are the band gap energy of the CdS nanoparticle and bulk respectively, and λ is the wavelength of absorbance. The absorbance at shorter wavelengths is attributed to the higher energetic transitions, giving its broad character. The strong PL implies that the surface states remain very shallow, it is reported that quantum yields of band edge will decrease exponentially with increasing depth of surface state energy levels [26].

In Fig. 6, we can see a peak at 365 nm, and since the particle size of CdS at 365 nm is lower than exciton Bohr radius, and according to the fact that the particle size cannot be less than the exciton Bohr radius, therefore, this peak appears due to either impurity or to unknown defect.

Photoluminescence study

Photoluminescence spectra of CdS nanoparticles in the present study indicates the presence of various types of defects.

Fig. 7, shows a wide variety of defects such as interstitial cadmium I_{Cd}^+ which act as donor levels, cadmium vacancy which act as acceptor levels V_{Cd}^- and lies near to the VB at $\sim 0.1-0.2$ eV [27], interstitial sulfur I_s^- , sulfur vacancy V_s^{2+} , and isolated cadmium vacancy V_{Cd}^{2-} who lies in the mid-gap region at $\sim 0.9-1.2$ eV from the VB edge [27, 28]. During the synthesis of CdS nanoparticles, the ratio between cadmium and sulfur salts was taken as 2:1.

From literatures [24, 29, 30], it was found that energy level corresponding to interstitial sulphur is near to valance band edge, and that corresponding to cadmium vacancy is at higher values than the interstitial sulphur. The emission peak observed at 502 nm ~ 2.47 eV can be ascribed to the radiative transition between cadmium interstitial band I_{Cd} and cadmium vacancy level V_{Cd} [9], which forms a Frenkel defect complex. The energy level diagram shown in the Fig. 7 illustrates the above transitions.

In general, the visible luminescence spectrum of CdS shows green, yellow, orange, and red emission. Where yellow emission is due to interstitial cadmium I_{Cd} , red emission is due to sulphur vacancy V_s [31, 32, 33]. The peak in the PL spectrum located around 543 ~ 2.28 eV is termed as green band luminescence. This peak arises due to interstitial sulphur sites I_s [34].

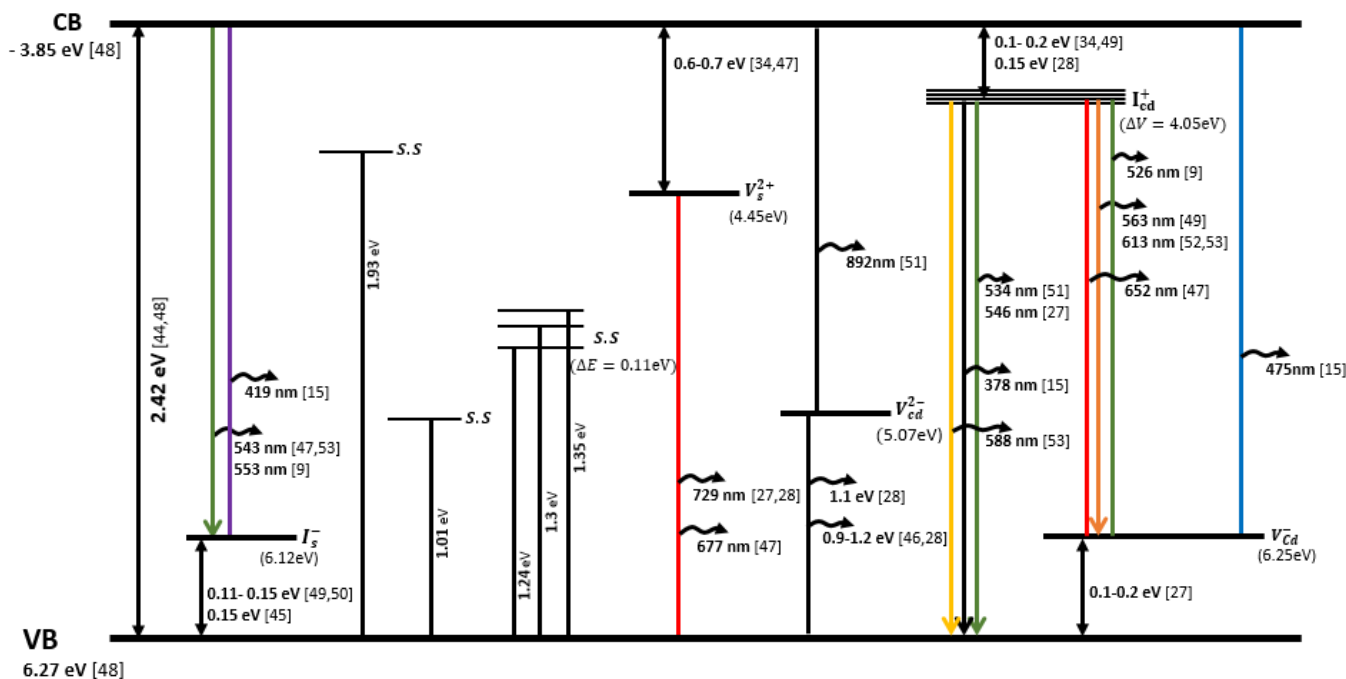


Fig. 7: Energy levels corresponding to different transitions in Photoluminescence of CdS.

FTIR

The result of Fourier Transform Infrared spectrum FTIR of CdS is presented in Fig 8. The results showed some absorption peaks in the region $4000-400cm^{-1}$, that is around 3429.2 , 1629.74 and $1110.92cm^{-1}$. In the higher energy region, the peak at $3429.2cm^{-1}$ is assigned to O-H stretching of absorbed water on the surface of CdS [35]. The peak at $1629.74cm^{-1}$ has corresponded to C-C bending vibration. It is believed that this peak was from surfactant used for capping agent which is Oleylamine OLA [36, 37]. Stretching vibration at absorption peak $1110.92cm^{-1}$ is related to silicon-oxy compounds (Si-O-C) [38].

The peak at $1400.22cm^{-1}$ has corresponded to bending vibration of methanol used in the process. It is also verified by its CH_3 -stretching vibrations occurring as very weak peaks just below $3000cm^{-1}$. The absorption peaks at 445.53 , 480.24 and $613cm^{-1}$ are corresponded to the stretching of S-S bond [39].

Stretching vibration of the Cd–S was reported as 405cm^{-1} [40], where the absorption peak was found at 412.74cm^{-1} . According to Kumar [41] dan Rusu [42], the peak of CdS was at 500cm^{-1} , while Karthik confirmed the vibration of Cd-S bonding at 601cm^{-1} [43]. When compared with this study, the CdS peak formed was slightly different. This is probably due to the different synthesis methods used.

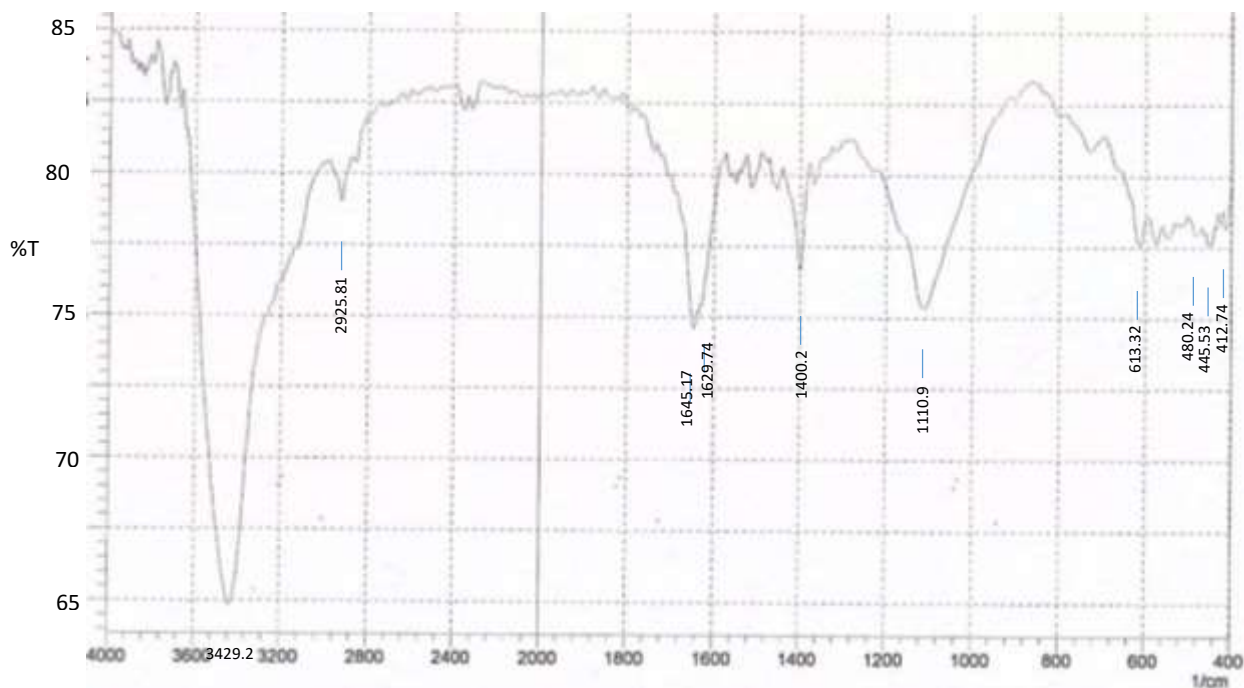


Fig. 8: FTIR spectra of CdS NPs

Conclusion

In this paper, we studied and characterized the point defects prepared by a chemical method and plot a scheme for most of the defects transitions that may happen.

In more details, we have successfully synthesized CdS nanoparticles by chemical method upon adding sulfide to a Cd with Oleylamine complex which act as a capping agent that passivate the nanoparticle surface and hence preventing bulk mineral precipitation. A rapid cooling was used to produce high concentration defects which in return affects the optical and structural properties of nanomaterials. It worth to mention that increasing defects leads to increase the size of CdS nanoparticles and forming new electronic states in the band gap. TEM result reveals that the CdS nanoparticles structures have irregular spherical shapes and are in contact with each other. Spherical nanoparticles were observed due to decrease the surface to volume ratio. X-ray diffraction (XRD) confirmed the wurtzite phase formation of CdS NPs. The average particle size of the CdS NPs is 5 nm and was calculated using different methods. The UV-vis absorption spectrum study reveals increasing the bang-gap of the CdS NPs (around 3 eV). This confirm the quantum confinement effect

References

- [1] Thambidurai, M. a., “Strong quantum confinement effect in nanocrystalline CdS”, *Journal of materials science*, 45(12), 3254-3258, (2010).
- [2] Kar, S. a., “Shape selective growth of CdS one-dimensional nanostructures by a thermal evaporation process”, *The Journal of Physical Chemistry B*, 110(10), 4542-4547, (2006).
- [3] Sivaraman, T. a., “Effect of magnesium incorporation on the structural, morphological, optical and electrical properties of CdS thin films”, *Materials science in semiconductor processing*, 27, 915-923, (2014).
- [4] Adnan Nazir, A. T., “Effect of Ag doping on opto-electrical properties of CdS thin films for solar cell applications”, *Journal of alloys and compounds*, 609, 40-45, (2014).
- [5] Singh Beer Pal, K. R., “Vacuum deposition of stoichiometric thin films of II-VI sulphide semiconductors”, *Physics Procedia*, 32, 766-771, (2012).

- [6] Moualkia, H. R., "The semiconducting properties of CdS nanocrystalline thin films prepared by chemical bath deposition", Application to the eosin photodegradation. *Journal of Materials Science: Materials in Electronics*, 28(24), 19105-19112, (2017).
- [7] Lin, C.-F. a.-Z.-M.-F., "CdS nanoparticle light-emitting diode on Si", *Light-Emitting Diodes: Research, Manufacturing, and Applications VI* (pp. 102-110), (2002).
- [8] Morales-Acevedo, A., "Thin film CdS/CdTe solar cells: research perspectives", *Solar Energy*, 80(6), 675-681, (2006).
- [9] Ramaiah, K. S.-K. , "Structural and optical investigations on CdS thin films grown by chemical bath technique", *Materials chemistry and physics*, 68(1-3), 22-30, (2001).
- [10] Lee, H. a., "Synthesis and characterizations of bare CdS nanocrystals using chemical precipitation method for photoluminescence application", *Journal of Nanomaterials*, 2009, (2009).
- [11] He, K. a., "Method for determining crystal grain size by x-ray diffraction", *Crystal Research and Technology*, 53(2), 1700157, (2018).
- [12] Kazmerski, L., "Polycrystalline and amorphous thin films and devices", (2012).
- [13] Rong, M. Z., "Surface modification and particles size distribution control in nano CdS/polystyrene composite film", *Chemical Physics*, 286(2-3), 267-276, (2003).
- [14] Devi, R Aruna and Latha, M and Velumani, S and Oza, Goldie and Reyes-Figueroa, P and Rohini, M and Becerril-Juarez, IG and Lee, Jae-Hyeong and Yi, Junsin, "Synthesis and characterization of cadmium sulfide nanoparticles by chemical precipitation method", *Journal of nanoscience and nanotechnology*, 15(11) 8434-8439, (2015).
- [15] Roshima, N. a., "Study on Vacancy Related Defects of CdS Nanoparticles by Heat Treatment", *Journal of Nano Research* (pp. 53-61), (2012).
- [16] Elilarassi, R. a., "Structural and optical characterization of CdS nanoparticles synthesized using a simple chemical reaction route", *Optoelectron. Adv. Mater*, 4, 309-312, (2010).
- [17] Waly, S. a., "Synthesis and characterization of CdS nanoparticles prepared by precipitation in the presence of span 20 as surfactant", *Russian Journal of Applied Chemistry*, 90(2), 292-297, (2017).
- [18] Ikhmayies, S. J.-B., "A study of the optical bandgap energy and Urbach tail of spray-deposited CdS:In thin films", *Journal of Materials Research and Technology*, 2(3), 221-227, (2013).
- [19] Dai, J. a., "The excitonic photoluminescence mechanism and lasing action in band-gap-tunable $CdS_{1-x}Se_x$ nanostructures", *Nanoscale*, 8(2), 804-811, (2016).
- [20] Mishra, S. K., "Structural, photoconductivity and photoluminescence characterization of cadmium sulfide quantum dots prepared by a co-precipitation method", *Electronic Materials Letters*, 7(1), 31-38, (2011).
- [21] Yadav, R. S., "Growth mechanism and optical property of CdS nanoparticles synthesized using amino-acid histidine as chelating agent under sonochemical process", *Ultrasonics sonochemistry*, 17(1), 116-122, (2010).
- [22] Kanemitsu, Y. a., "Photoluminescence spectrum of highly excited single CdS nanocrystals studied by a scanning near-field optical microscope", *Applied physics letters*, 81(1), 141-143, (2002).
- [23] Ishizumi, A. a., "Photoluminescence properties of single Mn-doped CdS nanocrystals studied by scanning near-field optical microscopy", *Applied Physics Letters*, 87(13), 133104, (2005).
- [24] Al-Douri, Y. a., "Optical investigations of blue shift in ZnS quantum dots", *Superlattices and Microstructures*, 88, 662-667, (2015).
- [25] Weller, H. a., "Photochemistry of colloidal semiconductors. Onset of light absorption as a function of size of extremely small CdS particles", *Chemical physics letters*, 124(6), 557-560, (1986).
- [26] Mullaugh, Katherine M and Luther III, George W, "Spectroscopic determination of the size of cadmium sulfide nanoparticles formed under environmentally relevant conditions", *Journal of Environmental Monitoring*, 12(4), 890-897, (2010).
- [27] Abken, A. E., "Photoluminescence study of polycrystalline photovoltaic CdS thin film layers grown by close-spaced sublimation and chemical bath deposition", *Journal of Applied Physics*, 105(6), 064515, (2009).

- [28] Varley, J. a., “Electrical properties of point defects in CdS and ZnS”, *Applied Physics Letters*, 103(10), 102103, (2013).
- [29] Zezza, F. a., “High quality CdS nanocrystals: surface effects”, *Synthetic Metals*, 139(3), 597-600, (2003).
- [30] Singh, V. a., “Structural and optical characterization of CdS nanoparticles prepared by chemical precipitation method”, *Journal of Physics and Chemistry of Solids*, 70(7), 1074-1079, (2009).
- [31] Chaure, S. a., “Stoichiometric effects on optical properties of cadmium sulphide quantum dots”, *IET Circuits, Devices and Systems*, 1(3), 215-219, (2007).
- [32] S. Wageh, Z. L.-R., “Reacciones de oxidación selectiva en Química Orgánica promovidas por la luz”, *Journal of Crystal Growth*, 255-332, (2003).
- [33] Nanda, J. a., “Sizable photocurrent and emission from solid state devices based on CdS nanoparticles”, *Applied physics letters*, 72(11), 1335-1337, (1998).
- [34] Vacuum deposition Aguilar-Hernandez, J. a.-P.-A.-G.-G.-L.-E.-C.-G.-C., “Photoluminescence and structural properties of cadmium sulphide thin films grown by different techniques”, *Semiconductor science and technology*, 18(2), 111, (2002).
- [35] Shivashankarappa, Aishwarya and Sanjay, KR, “Study on biological synthesis of cadmium sulfide nanoparticles by *Bacillus licheniformis* and its antimicrobial properties against food borne pathogens “, *Nanoscience and Nanotechnology Research*, 3(1), 6-15, (2015).
- [36] Schulz, Hartwig and Baranska, Malgorzata, “Identification and quantification of valuable plant substances by IR and Raman spectroscopy”, *Vibrational Spectroscopy*, 43(1), 13-25, (2007).
- [37] Dovbeshko, Galina I and Gridina, Nina Ya and Kruglova, Elena B and Pashchuk, Olena P, “FTIR spectroscopy studies of nucleic acid damage”, *Talanta*, 53(1), 233-246, (2000).
- [38] Coates, John, “Interpretation of infrared spectra, a practical approach”, (2007).
- [39] Nandiyanto, Asep Bayu Dani and Oktiani, Rosi and Ragadhita, Risti, “How to read and interpret FTIR spectroscopy of organic material”, *Indonesian Journal of Science and Technology*, 4(1), 97-118, (2019).
- [40] Sun, Z.-B. a.-Z.-Q.-M., “Two-and three-dimensional micro/nanostructure patterning of CdS--polymer nanocomposites with a laser interference technique and in situ synthesis. *Nanotechnology*”, 19(3), 035611, (2007).
- [41] Kumar, N. a., “Spin coating of highly luminescent Cu doped CdS nanorods and their optical structural characterizations”, *Chalcogenide Lett*, 12(6), 333-338, (2015).
- [42] Rusu, M. a., “CdS/ZnS-doped silico-phosphate films prepared by sol-gel synthesis”, *Journal of Non-Crystalline Solids*, 481, 435-440, (2018).
- [43] Karthik, K. a., “Microwave-assisted bioengineered CdS nanoparticles for photocatalytic and biological applications”, *Catalytica*, 1(1), 40-50, (2019).
- [44] Jassim, S. A.-J., “Influence of substrate temperature on the structural, optical and electrical properties of CdS thin films deposited by thermal evaporation”, *Results in Physics*, 173-178, (2013).
- [45] Kulp, B. a., “ Displacement of the sulfur atom in CdS by electron bombardment”, *Journal of Applied Physics*, 31(6), 1057-1061, (1960).
- [46] Susa, N. a., “Effects of annealing in Cd or S vapor on photoelectric properties of CdS single crystals”, *Japanese Journal of Applied Physics*, 15(12), 2365, (1976).
- [47] Vigil, O. a.-R.-A., “Characterization of defect levels in chemically deposited CdS films in the cubic-to-hexagonal phase transition”, *Journal of Vacuum Science and Technology A: Vacuum, Surfaces, and Films*, 15(4), 2282-2286, (1997).
- [48] Septina, W. a., “Photosplitting of water from wide-gap Cu (In, Ga) S₂ thin films modified with a CdS layer and Pt nanoparticles for a high-onset-potential photocathode”, *The Journal of Physical Chemistry C*, 119(16), 8576-8583, (2015).
- [49] Narayanam, P. K., “Effect of heat treatment on the photoluminescence of CdS nanocrystallites in cadmium-rich organic Langmuir Blodgett matrix”, *Materials Chemistry and Physics*, 139(1), 196-209, (2013).
- [50] Achour, S. a., “Effect of thermal annealing on the cathodoluminescence of evaporated CdS films”, *Thin solid films*, 144(1), 1-6, (1986).

- [51] Meher, S. a., "Native defects in sol-gel derived CdS buffer layers for photovoltaic applications", *Journal of Materials Science: Materials in Electronics*, 28(8), 6033-6046, (2017).
- [52] Gutu, T. a.-h., "Electron microscopy and optical characterization of cadmium sulphide nanocrystals deposited on the patterned surface of diatom biosilica", *Journal of Nanomaterials*, 2009, (2009).
- [53] De Azevedo, W. a., "A new and straightforward synthesis route for preparing Cds quantum Dots", *Journal of luminescence*, 132(7), 1740-1743, (2012).